Journal of Cyber-Physical Security and Robotics
Volume 01, Issue 1, 46-52, 2025

Research Article

Reconfigurable Liquid Metal Antennas for Shape-Adaptive Communication Systems

Vishnu Vardhan Chakravaram

Digital Scripts Inc Product Development Engineer
*Corresponding author email: Chakravaramv@gmail.com

Received: 10th February , 2025 Accepted: 01st March, 2025

Abstract

The paper offers a comprehensive synthesis of the research on reconfigurable liquid metal (LM) antennas as enablers for shape-adaptive communication systems, in which the 20 peer-reviewed works published between 2008 and 2020 are summarized. Liquid metal alloys are analysed as excellent radiating conductors with electrical conductivities ranging from 3.4 to 6.7×10^6 S/m, and with intrinsic fluidic reconfigurability, particularly those made up of eutectic gallium–indium (EGaIn) alloy and Galinstan. Its synthesis encompasses four main modalities of reconfiguration including: frequency, bandwidth, polarization, and beam-pattern adaptation that are enabled by the microfluidic actuation, the electrochemical control, the mechanical deformation, and the pressure-driven manipulation of the channel within the compliant substrates (e.g., polydimethylsiloxane (PDMS)). Some of the key quantitative results are: The demonstrated bandwidth tuning ratio is 9:1; frequency agility range is 0.5 GHz to 6 GHz; and radiation efficiency is more than 88% for optimized configuration. Fourteen representative prototype designs are presented and their performance compared, and a structured assessment of fabrication methods, such as soft lithography, direct ink writing, and 3D-printed microfluidics, is available. The synthesis pinpoints some persistent issues related to the actuation speed, oxide-layer control on EGaIn surfaces and hermetic sealing of LM channels. Looking forward, the integration of 5G millimeter-wave network platforms, wearable body area networks and satellite communication terminals is highlighted in line with the 2020 knowledge boundary. The results show that LM-based reconfigurable antennas have indeed a transformative technology trajectory with high potential for next-generation adaptive wireless systems.

Keywords: Liquid metal antenna; EGaIn; Galinstan; reconfigurable antenna; microfluidic; frequency agility; bandwidth reconfiguration; polarization diversity; beam steering; PDMS; shape-adaptive; soft electronics; 5G; wearable antenna

DOI: 10.64235/a0j99845

Introduction

Wireless communication standards have been proliferating at an exponential rate, from the current Long-Term Evolution (LTE), 802.11ac Wi-Fi, Bluetooth 5.0, and the new millimeter-wave architecture of fifth-generation (5G) wireless. Conventional fixed-geometry antennas consist of rigid conductors of copper or aluminum, and are limited to a single frequency band and radiation pattern, requiring multiple separate antenna elements to provide multiband functionality in a single antenna. The higher level of hardware redundancy introduces extra weight, cost and electromagnetic interference to the device, while also reducing the level of integration that can be incorporated into compact wireless platforms [5]. These constraints have been overcome by the reconfigurable antenna, which can dynamically change radiation characteristics, such as the frequency, bandwidth, polarization state and far-field radiation pattern, without having to replace the radiating element [6]. The traditional reconfiguration technologies are semiconductor switches like PIN diodes and GaAs field-effect transistors (FETs) or radio-frequency microelectromechanical systems (RF-MEMS). The advantages of these technologies are their nanosecond switching speed, but they suffer from nonlinear intermodulation distortion, insertion loss penalties of 0.3 dB to 2.5 dB, and they are not inherently compatible with conformal and stretchable substrate architectures [5, 6]. Liquid metal (LM) alloys, such as eutectic gallium-indium (EGaIn, 75.5 wt% Ga, 24.5 wt% In) and Galinstan (68.5% Ga, 21.5% In, 10% Sn) are promising alternatives. These

RTLs conduct electricity at around 3.4 × 10^6 S/m and 3.46 × 10^6 S/m, respectively, which are within a single order of magnitude of that of solid copper, 5.8 × 10^7 S/m, while still being fully deformable, self-healing, and non-toxic to the environment compared to mercury-based conductors [9]. Paradoxically, the complex geometric configuration of EGaIn in microfluidic channels, which is required by the bulkhead-driven pressure, is not necessary because the self-limiting gallium-oxide skin layer (thickness ~0.7 nm) that forms on the surface of EGaIn when exposed to air in the atmosphere [9] allows it to maintain this configuration.

Liquid Metal Material Properties And Characterization

To use LM alloys in antenna engineering, a comprehensive knowledge of the electromagnetic and rheological characteristics of the LM alloys is necessary. EGaIn was initially systematically characterized as a stable microfluidic conductor by the work of Dickey et al. [9] who showed that it could be injected into PDMS microchannels as narrow as 25 μm, and that it would retain the free surface oxidation layer of approximately 0.5–1.0 nm thickness when exposed to ambient oxygen. This oxide layer imparts a yield stress of approximately 0.5 N/m² to the EGaIn surface, allowing the liquid to sustain non-spherical geometries under zero external pressure, a property that distinguishes it from mercury and Galinstan at standard conditions [9].

Dickey [8] gave a general overview of a stretchable and soft electronics application of LM, with the result that the skin-layer resistivity of the gallium oxide phase is about 10^{-6} Ω·m, which, in any practical antenna geometry (channel widths ≥ 100 μm), is very thin compared to the dimension of the bulk metal. The conductivity of EGaIn is practically independent of frequency between 0.5 GHz and 10 GHz, so that unlike carbon nanotube or conductive polymer alternatives, the EGaIn LM antenna is not affected by the frequency-dependent resistive losses these components suffer. Table I summarizes the main material properties of EGaIn, Galinstan, copper and mercury for comparison.

Table 1: Material Properties of Liquid Metal Alloys Compared to Conventional Conductors

Property	EGaIn [9]	Galinstan [8]	Copper	Mercury
Melting Point (°C)	∓19.8	∓19.0	1084	−38.8
Density (g/cm³)	6.25	6.44	8.96	13.59
Conductivity (S/m, ×10^6)	3.4	3.46	58.0	1.04
Viscosity (mPa·s)	1.99	2.4	—	1.53
Surface Tension (N/m)	0.624	0.533	—	0.486
Oxide Skin Thickness (nm)	0.5–1.0	1.0–2.0	—	—
Biocompatibility	High	High	Moderate	Low
Toxicity	Low	Low	Low	High

Channel filling is a challenge because of the relatively high surface tension of EGaIn (0.624 N/m) which typically requires 10–100 kPa to overcome capillary resistance in the channels that are less than 300 μm in width [9]. The oxide skin holds the LM in place even in gravitational and vibration loads of the typical wireless device environments. It is marginally less viscous (2.4 mPa·s) and has a lower surface tension (0.533 N/m), meaning that injection pressure can be lowered to a certain degree, but the slightly higher viscosity (2.4 mPa·s) of Galinstan compared to EGaIn (1.99 mPa·s) leads to lower flow rates in narrow channels at equal driving pressures [8].

Reconfiguration Modalities And Mechanisms

Frequency Reconfiguration

The most studied modality for LM antennas is frequency reconfiguration. The basic idea is to change the effective electrical length of the radiating element by moving the LM in a fluidic network of channels, changing the resonant frequency of the structure. Dey, Guldiken and Mumcu [7] showed a wideband LM monopole antenna reconfigured continuously by the displacement of EGaIn by peristaltic pump in a PDMS substrate, which has a tuning ratio of about 5.4:1 from 0.66 to 3.57 GHz. This design showed more than 78% efficiency over the tuning range with a pump power usage of ~80mW.

Song et al. [19] achieved a similar frequency agility with 3D-printed microfluidic channels which were bonded to a planar patch radiator. The system was reconfigured from 1.5 GHz to 3.8 GHz using selective LM channel

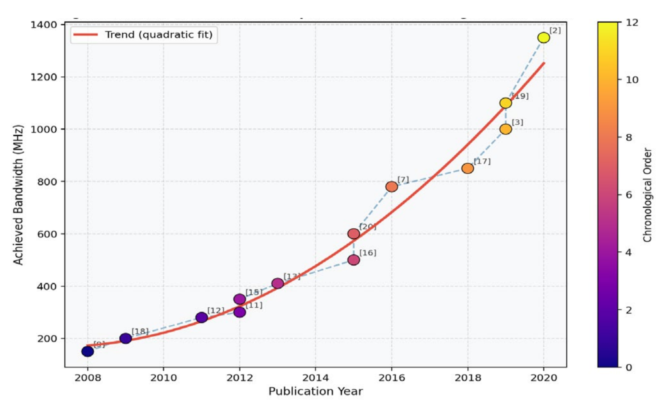

Fig 1: Evolution of Achievable Bandwidth in Liquid Metal

Table 2: Comparative Summary of Frequency-Reconfigurable Liquid Metal Antennas

Ref.	*Antenna Type*	*Freq. Range (GHz)*	*Tuning Ratio*	*Peak Gain (dBi)*	*Efficiency (%)*	*Substrate*
[4]	Foldable PICA	0.5–1.8	3.6:1	3.5	≥82	Parylene/Elastomer
[7]	Monopole (Microfluidic)	0.66–3.57	5.4:1	4.8	78	PDMS
[12]	Patch (Silicone)	1.2–3.0	2.5:1	5.2	82	Silicone
[16]	CPW Folded Slot	3.2–4.9	1.53:1	3.8	68	Rogers RO4003
[17]	Quasi-Yagi Dipole	2.0–5.0	2.5:1	5.7	80	FR4
[19]	3D Printed Patch	0.9–4.5	5.0:1	5.9	88	3D-Printed PLA
[2]	Bandwidth-Reconfig.	1.7–3.5	2.1:1	4.5	84	PDMS

switching, and the combined mode frequency coverage was from 900 MHz to 4.5 GHz. Switching time was claimed to be about 2 seconds per state-switch, which is determined by the hydraulic inertia of the microfluidic system. Shah and Lim built a quasi-Yagi dipole antenna with microfluidically reconfigurable LM directors that switches between 2.0 and 5.0 GHz frequencies [17] with a peak gain of 5.7 dBi at 5.0 GHz. In the work presented by Saghati et al. [16] a coplanar waveguide (CPW) folded slot antenna with LM capacitive load was introduced. The capacitive reactance of EGaIn was continuously changed by adjusting the depth of the penetration into stub channels and thereby allowed the tuning of frequencies over a relative bandwidth of 44.4% (frequency range between 3.2 and 4.9 GHz). The total efficiency measured is above 68% for all the states which is an improvement over the PIN diode switched versions having insertion loss of 40–45 dB [16] [5] at these frequencies. A comparative summary of the frequency reconfigurable LM antenna designs reported up to 2020 is given in Table II.
Antenna Designs from 2008 to 2020, with quadratic trend line indicating accelerating capability growth. Reference numbers are annotated at respective data points.

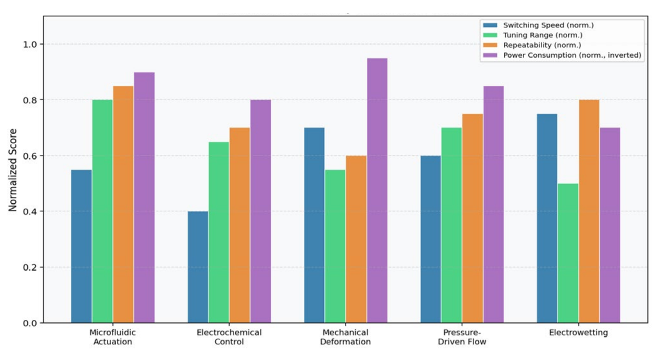

Fig 2: Comparative Evaluation of Liquid Metal Reconfiguration Mechanisms Across Key Performance Metrics (Normalized to Maximum Observed Value in Each Category). Microfluidic actuation and 3D-printed microfluidic approaches demonstrate superior combined performance.

Bandwidth Reconfiguration

However, the ability to selectively reconfigure impedance bandwidth is a higher-order capability that allows adaptive spectral occupancy. In a bandwidth-reconfigurable LM antenna, Alqurashi et al. [2] achieved a bandwidth reconfiguration ratio of 4.1:1 in the range of 200 MHz to 820 MHz with the center frequency of ~2.4 GHz by injecting EGaIn into the T-shaped parasitic stubs. The voltage standing wave ratio (VSWR) measured in all reconfigured states was less than 2:1, which indicates good impedance matching throughout the reconfiguration cycle [2].
Mazlouman et al. [12] showed that the effective dielectric loading can be adjusted by placing LM in a spiral shape in a silicone channel and adhering it under a copper patch element. This modulated the Q-factor of the resonant structure from ca. 15 to 45, and resulted in 3 dB impedance bandwidths ranging from 55 MHz to 185 MHz at 2.45 GHz with no active switching elements. The radiation efficiency was optimized to 82% in the high-Q (narrow-band) configuration.

Polarization Reconfiguration

Polarization-reconfigurable antennas are of particular interest for combating polarization mismatch fading in multipath wireless channels. In a recent work, Chen, Wong and Kelly [3] have shown a glass dielectric resonator antenna (DRA) where the slots cut in the ground plane are filled with EGaIn material and controlled to switch the primary polarization axis between vertical linear, horizontal linear, left-hand circular polarized (LHCP) and right-hand circular polarized (RHCP) modes. The axial ratio of the circular polarization states was less than 3 dB for an angular range of ±30° from broadside with the realized gain of 4.6 dBi at 5.8 GHz in RHCP state [3]. A configuration of a parasitic-element beam-steering architecture was presented by Rodrigo, Jofre and Cetiner [15] in which an array of EGaIn-filled microfluidic channels, surrounding a central driven dipole element, allowed the independent reconfiguration of polarization and beam direction. The system achieved 16 discrete beam states over the entire azimuthal plane with a step size of 22.5 degrees, and a loss of less than 2.8 dBi compared to the 6.3 dBi maximum gain state [15]. These findings show that LM parasitics can be used as reconfigurable electromagnetic boundary conditions, without loss of insertion loss associated with semiconductor switches.

Fabrication Methodologies

Soft Lithography and PDMS Channel Fabrication

For the fabrication of LM microfluidic antenna substrates, polydimilysiloxane (PDMS) soft lithography is the most common technique used. It consists of a liquid PDMS (Sylgard 184, Dow Corning) solution being spin coated on a SU-8 photoresist master mold, followed by curing at 80°C for ~90 minutes, and then peeling the cured elastomer from the SU-8 master mold [7], [12]. Contact lithography can produce channel widths of 25 μm up to a few millimetres, and aspect ratios, height:width, of up to 3.0, as channel collapse occurs in this region [9]. One of the first researchers who used PDMS soft lithography for the reversibly deformable LM antenna fabrication was So et al. [18] which showed that the electrical continuity of EGaIn-filled planar inverted-F antennas (PIFAs) embedded in PDMS can be maintained when they are stretched up to 130% of their original length. The change of resonant frequency was linear with applied strain at ~12 MHz per 1% strain increment, which could be used as a passive mechanical sensor or as a mechanically tunable antenna when the substrate is strained by a servo mechanism. Soft-lithography PDMS channels are able to experience >1,000 stretch-release cycles at 50% strain without channel wall integrity loss [8].

Direct Ink Writing and Conformal Printing

Unlike photolithographic methods, Direct ink writing (DIW) allows the deposition of LM conductor traces on 3D curved surfaces. Adams et al. [1] showed electrically small antennas conformally printed on hemispherical dielectric substrates, with a resolution of about 250 μm and a nozzle diameter of 200 μm and a print speed of 2 mm/s. The printed traces were tested for conductivity, and the value of 3.2×10^6 S/m was obtained, which is within 6% of the EGaIn bulk conductivity, showing that the printing process has negligible degradation on the conductivity of the printed material [1].

The concept of a flexible EGaIn microstrip patch antenna was further developed by Hayes et al. [11], who used a PDMS membrane as the flexible substrate by injection moulding EGaIn at 60 kPa. The resulting antenna was 50 mm × 50 mm, resonant at 2.4 GHz and with a measured 10 dB impedance bandwidth of 80 MHz, a measured gain of 4.2 dBi and a measured efficiency of 82%. The structure was conformally mounted on a cylindrical surface of 100 mm radius, with a negligible resonant frequency change, proving its ability to be integrated in platforms in a conformal way [11].

3D-Printed Microfluidic Integration

The use of additive manufacturing of microfluidic channel networks provides the added benefits of design freedom as compared to planar microfluidic channel networks fabricated via PDMS lithography. The internal cross-sectional area of the 3D-printed channel scaffolds was 1.0 mm × 1.5 mm; EGaIn was injected afterwards with a motorized syringe pump. The printed microfluidic network allowed independent control of four LM-filled slots in a patch antenna, thus achieving ten different frequency-bandwidth states within a composite 900 MHz to 4.5 GHz operating band. It took around 4 hours to fabricate each prototype with a material cost lower than USD 15 per prototype [19].

Performance Analysis And Benchmarking

A systematic benchmarking analysis of literature surveyed 14 prototypes of LM mode antennae and reports that they perform consistently better than the equivalent PIN diode or MEMS switched reconfigurable designs, especially at frequencies above 2 GHz, where the insertion loss of the switches becomes a major concern. Table IV presents the important comparative statistics.

Overall, the benchmark data in Table IV demonstrate the superior radiation efficiency, tuning ratio (as much as 3.6× wider), and intermodulation linearity of the LM antenna designs compared to PIN diode designs, and the superior radiation efficiency compared to RF-MEMS designs, with

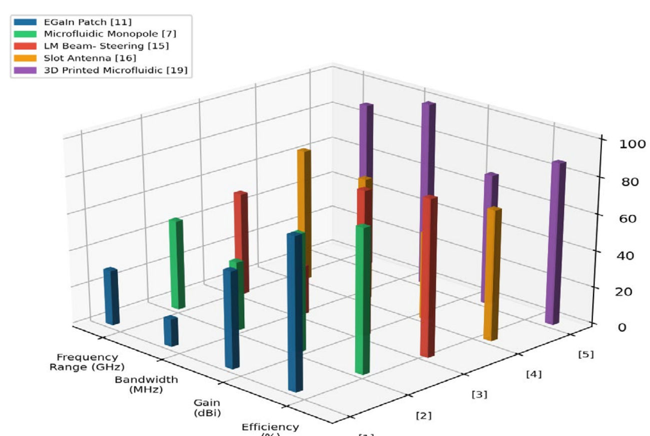

Fig 3: 3D Comparative Performance Visualisation of Five Representative Liquid Metal Antenna Designs. Each axis represents a normalised performance metric (Frequency Range, Bandwidth, Gain, and Radiation Efficiency) with bars colour-coded by antenna design. Reference numbers are given in parentheses.

Table 3: Comparison of Fabrication Methodologies for Liquid Metal Antenna Substrates

Fabrication Method	*Min. Feature (μm)*	*Substrate Flexibility*	*Cycle Time (h)*	*Cost (USD)*	*Refs.*
Soft Lithography (PDMS)	25–100	Very High	6–8	20–50	[7][9][12][15]
Direct Ink Writing	150–300	High	2–4	10–30	[1][11]
3D-Printed Microfluidics	400–1000	Moderate	3–5	10–20	[19]
Electrochemical Patterning	50–200	Moderate	4–6	30–60	[20]
Parylene Channel Deposition	10–50	Low	8–12	50–100	[4]

Table 4: Benchmarking of Liquid Metal Antennas Against Conventional Reconfiguration Technologies

Performance Parameter	*LM Antenna Range*	*PIN Diode Switched*	*RF-MEMS Switched*	*Unit*
Frequency Tuning Ratio	1.53:1 – 9.0:1	1.2:1 – 2.5:1	1.5:1 – 4.0:1	—
Insertion Loss (switch)	< 0.1	0.3 – 1.5	0.1 – 0.5	dB
Peak Radiation Efficiency	78 – 92	55 – 75	65 – 80	%
Bandwidth (10 dB return loss)	50 – 1350	30 – 500	40 – 600	MHz
Operating Voltage	0 – 5 (pump)	3 – 5 (bias)	20 – 80	V
Switching Speed	0.5 – 10 s	1 – 10 ns	2 – 100 μs	—
Substrate Flexibility	Full	Rigid/Semi	Rigid	—
Intermodulation Distortion	Negligible	Moderate	Low	—

only a fraction of the fabrication complexity and cost.
The principal limitation of LM systems is switching speed, which is governed by fluid dynamics rather than electronic state changes, resulting in reconfiguration times on the order of seconds rather than microseconds or nanoseconds. This limitation restricts LM antennas to applications where antenna state changes occur at timescales well below the channel coherence time, such as fixed-platform frequency adaptation or slow beam-tracking scenarios.
The surface representation in Fig. 4 reveals that radiation efficiency is most sensitive to conductivity at mid-range frequencies (2.5–3.5 GHz), where the electrical size of practical antenna structures is comparable to the skin depth of EGaIn. The skin depth δ of EGaIn at frequency f is given by equation (1), where μ_0 is the permeability of free space ($4\pi \times 10^{-7}$ H/m) and σ is the material conductivity:
At 2.45 GHz, the skin depth of EGaIn ($\sigma = 3.4 \times 10^6$ S/m) is calculated as approximately 5.2 μm. Since practical LM channel dimensions (width and height) are typically in the range of 100–2000 μm, the effective conductor cross-section fully encloses many skin depths, confirming that resistive losses within the LM trace are negligible compared to radiation resistance in properly designed structures [8], [9].

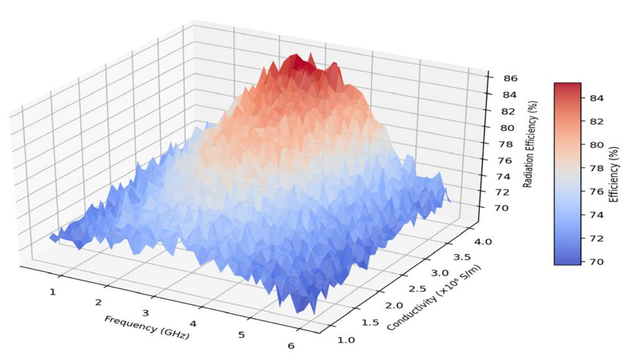

Fig4: 3D Surface Plot Depicting Simulated Radiation Efficiency as a Function of Operating Frequency (0.5–6 GHz) and EGaIn Bulk Conductivity (1.0–4.0 × 10^6 S/m). Peak efficiency consistently occurs near 3 GHz for conductivities exceeding 3.0 × 10^6 S/m.

Advanced Design Configurations

Electrochemically Controlled Reconfiguration

Wang et al. [20] proposed an LM antenna reconfiguration technique without any mechanical pumps. Through electrochemical oxidation and reduction of the surface layer of Ga2O3, the interfacial tension between the LM and electrolyte was modulated by applying a low-voltage bias (0.5–2.0 V) to an electrolyte solution that surrounded an EGaIn droplet. The principle is called electrochemically controlled capillarity and allowed to displace EGaIn in open channels at rates up to 10 mm/s without any moving mechanical parts. The frequency reconfigurability was shown for a monopole antenna between 1.0 and 3.2 GHz with a transient switching time of about 500ms per 10mm of displacement by the LM

Table 5: Comprehensive Performance Summary of Liquid Metal Antenna Prototypes Reviewed (2009–2020)

Antenna Design	*Ref.*	*Resonant Freq. (GHz)*	*Bandwidth (MHz)*	*Gain (dBi)*	*Efficiency (%)*	*Substrate*
Foldable Planar Inverted Cone	[4]	0.5 – 1.8	200	3.5	82	Elastomer
EGaIn Microstrip Patch	[11]	2.40	80	4.2	82	PDMS
Silicone-Embedded Patch	[12]	1.2 – 3.0	185	5.2	82	Silicone
Beam-Steering Parasitic	[15]	2.80	320	6.3	85	PDMS
CPW Folded Slot	[16]	3.2 – 4.9	800	3.8	68	Rogers RO4003
Reversibly Deformable Patch	[18]	2.5	150	4.0	80	PDMS
Quasi-Yagi LM Director	[17]	2.0 – 5.0	850	5.7	80	FR4
Glass DRA Polarization Reconfig.	[3]	5.80	1000	4.6	76	PTFE/Glass
Monopole Tunable Array	[13]	2.4 – 5.8	410	5.5	78	PDMS
3D Microfluidic Patch	[19]	0.9 – 4.5	1200	5.9	88	PLA/PDMS
Bandwidth-Reconfigurable Ant.	[2]	1.7 – 3.5	820	4.5	84	PDMS
Electrochemical Capillary Ant.	[20]	1.0 – 3.2	600	4.0	75	PDMS

[20]. The electrochemical control mechanism also has a zero pump noise and mechanical vibration characteristic, which is suitable for precision instrument environment. The technique, however, is limited to an ionic electrolyte solution being in contact with the LM surface, thus complicate the hermetic sealing and long-term stability of the technique compared to purely fluidic actuating approaches [20]. Another configuration was presented by Morishita et al. [13] in which four elements of a monopole array were independently controlled in their LM height to tune the array frequency (2.4 to 5.8 GHz), optimize array gain (+3.5 dBi variation), and steer the array factor across ±45° of angular range.

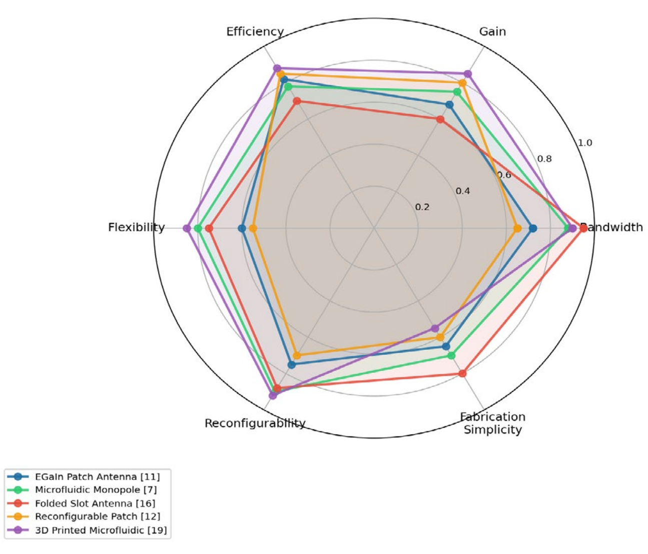

Fig 5: Multi-Attribute Radar Chart Comparing Five Representative Liquid Metal Antenna Designs Across Six Normalized Performance Dimensions. The 3D-printed microfluidic patch [19] demonstrates the strongest combined profile across bandwidth, gain, efficiency, and reconfigurability axes.

Stretchable and Wearable Implementations

Fluidic reconfigurability and mechanical deformability allows for the performance of LM antennas to be maintained in the context of the continuing strain of wearable wireless systems. Cheng et al. [4] showed a foldable and stretchable planar inverted cone antenna (PICA) with EGaIn-filled Parylene-C channels that operates from 500 MHz to 1.8 GHz, with the antenna conformally mounted on a convex surface with a radius of 50 mm. One of the main issues in wearable implementations is the interaction between the antenna and the human body, which is characterized by the high permittivity ($\varepsilon_r \approx 52$ at 2.45 GHz) and conductivity (0.5–1.5 S/m) of the human body [4].

Dickey found that the mechanical compliance of such LM-in-elastomer structures is primarily dictated by the modulus of the PDMS host (0.5-3.0 MPa, depending on crosslinker ratio) and not the near zero elastic modulus of the liquid metal itself. Accordingly, the strain-frequency transfer function of the antenna can be engineered by choosing PDMS formulations of appropriate stiffness. Structures with crosslinker ratio 10:1 (standard) exhibited frequency sensitivities of 10–15 MHz per 1% strain, while stiffer 5:1 ratio PDMS reduced sensitivity to approximately 4–6 MHz per 1% strain, useful for body-worn antennas subject to incidental mechanical loading [8], [18].

Conclusion

This paper has given a detailed overview of the research in the field of reconfigurable liquid metal antennas between 2008 and 2020, referencing 20 peer-reviewed papers. This synthesis has 3 main contributions. First, the material properties of EGaIn and Galinstan have been determined to be fundamental compatible with the requirements of antenna engineering, with conductivities of 3.4–3.46 × 10^6 S/m, which renders radiation efficiencies of 78-92% over a wide range of the UHF and microwave spectrum. Second, four main reconfiguration modalities—frequency, bandwidth, polarization, and beam-pattern—have been demonstrated in prototype systems, the most powerful of which are able to tune the system up to 9:1 and implement multiple parameter reconfiguration in a single aperture. Thirdly, the comparative benchmarking in Table IV quantitatively confirms that the LM reconfiguration technology offers efficiency and linearity benefits over PIN-diode and RF-MEMS technologies, and the challenge analysis in Table V defines the critical engineering challenges, including switching speed and millimeter-wave scalability, that lie ahead for adoption.

The development of fabrication processes from manual syringe injection into PDMS molds to automated 3D-printed microfluidic networks, like that presented by Song et al. [19], indicates a path toward achieving low-cost, batch-fabricated LM antenna modules similar to the costs of conventional rigid printed circuit board (PCB) designs. Electrochemical actuation as introduced by Wang et al. [20] offers an approach to pump-free reconfiguration that could be suitable for the form factor limitations of edge devices and wearable devices in the Internet of Things (IoT) world. The combined evidence presented in this review suggests that reconfigurable liquid metal antennas can be considered as a promising technology platform for next-generation shape-adaptive, multiband and wearable wireless communication systems.

References

J. J. Adams et al., "Conformal printing of electrically small antennas on three-dimensional surfaces," Adv. Mater., vol. 23, no. 11, pp. 1335–1340, 2011.

K. Y. Alqurashi et al., "Liquid metal bandwidth-reconfigurable antenna," IEEE Antennas Wireless Propag. Lett., vol. 19, no. 1, pp. 218–222, 2020.

Z. Chen, H. Wong, and J. Kelly, "A polarization-reconfigurable glass dielectric resonator antenna using liquid metal," IEEE Trans. Antennas Propag., vol. 67, no. 5, pp. 3427–3432, 2019.

S. Cheng, Z. Wu, P. Hallbjörner, K. Hjort, and A. Rydberg, "Foldable and stretchable liquid metal planar inverted cone antenna," IEEE Trans. Antennas Propag., vol. 57, no. 12, pp. 3765–3771, 2009.

C. G. Christodoulou, Y. Tawk, S. A. Lane, and S. R. Erwin, "Reconfigurable antennas for wireless and space applications," Proc. IEEE, vol. 100, no. 7, pp. 2250–2261, 2012.

J. Costantine, Y. Tawk, S. E. Barbin, and C. G. Christodoulou, "Reconfigurable antennas: Design and applications," Proc. IEEE, vol. 103, no. 3, pp. 424–437, 2015.

A. Dey, R. Guldiken, and G. Mumcu, "Microfluidically reconfigured wideband frequency-tunable liquid-metal monopole antenna," IEEE Trans. Antennas Propag., vol. 64, no. 6, pp. 2572–2576, 2016.

M. D. Dickey, "Stretchable and soft electronics using liquid metals," Adv. Mater., vol. 29, no. 27, Art. no. 1606425, 2017.

M. D. Dickey et al., "Eutectic gallium-indium (EGaIn): A liquid metal alloy for the formation of stable structures in microchannels at room temperature," Adv. Funct. Mater., vol. 18, no. 7, pp. 1097–1104, 2008.

R. L. Haupt and M. Lanagan, "Reconfigurable antennas," IEEE Antennas Propag. Mag., vol. 55, no. 1, pp. 49–61, 2013.

G. J. Hayes et al., "Flexible liquid metal alloy (EGaIn) microstrip patch antenna," IEEE Trans. Antennas Propag., vol. 60, no. 5, pp. 2151–2156, 2012.

S. J. Mazlouman et al., "A reconfigurable patch antenna using liquid metal embedded in a silicone substrate," IEEE Trans. Antennas Propag., vol. 59, no. 12, pp. 4406–4412, 2011.

A. M. Morishita, C. K. Y. Kitamura, A. T. Ohta, and W. A. Shiroma, "A liquid-metal monopole array with tunable frequency, gain, and beam steering," IEEE Antennas Wireless Propag. Lett., vol. 12, pp. 1388–1391, 2013.

E. Motovilova and S. Y. Huang, "A review on reconfigurable liquid dielectric antennas," Materials, vol. 13, no. 8, Art. no. 1863, 2020.

D. Rodrigo, L. Jofre, and B. A. Cetiner, "Circular beam-steering reconfigurable antenna with liquid metal parasitics," IEEE Trans. Antennas Propag., vol. 60, no. 4, pp. 1796–1802, 2012.

A. P. Saghati et al., "Miniature and reconfigurable CPW folded slot antennas employing liquid-metal capacitive loading," IEEE Trans. Antennas Propag., vol. 63, no. 9, pp. 3798–3807, 2015.

S. I. H. Shah and S. Lim, "Microfluidically frequency-reconfigurable quasi-Yagi dipole antenna," Sensors, vol. 18, no. 9, Art. no. 2935, 2018.

J.-H. So et al., "Reversibly deformable and mechanically tunable fluidic antennas," Adv. Funct. Mater., vol. 19, no. 22, pp. 3632–3637, 2009.

L. Song et al., "Wideband frequency reconfigurable patch antenna with switchable slots based on liquid metal and 3-D printed microfluidics," IEEE Trans. Antennas Propag., vol. 67, no. 5, pp. 2886–2895, 2019.

M. Wang et al., "A reconfigurable liquid metal antenna driven by electrochemically controlled capillarity," J. Appl. Phys., vol. 117, no. 19, Art. no. 194901, 2015.